CONDUCTIVITY IN THE DISTORTED ONE-DIMENSIONAL ELECTRON SYSTEM*

By B. R. Bułka

Ferromagnetic Laboratory, Institute of Molecular Physics, Polish Academy of Sciences, Poznań**

(Received May 11, 1979)

Distorted atomic chain is described in the tight binding approximation. For this system, using the Green functions method the dynamical electrical conductivity is calculated exactly.

1. Introduction

One-dimensional, or more correctly, quasi-one-dimensional crystals are experimentally and theoretically extensively studied [1]. The physical properties of these systems very often show peculiar features and anomalies, existence of an insulator — metal like transition, structural and magnetic transitions. From theoretical point of view one-dimensional electron systems are unstable and the Peierls instability, the charge density wave (CDW) or the spin density wave is often considered (see e.g. [1, 2]). If in the system the distortion of the atomic chain (the Peierls distortion) appears then electron hopping integrals are modulated with a period of the distortion. However, the modulation of the hopping integrals may be due not only to the lattice modulation. For example, in TCNQ salts with asymmetric donors we expect that ordered donor chains modulate electron hopping integrals in an acceptor chain, as well. Thus, the electronic band structure may be analogical in both cases, but in the latter case the chain is undistorted. We distinctly differentiate these two models (see also [3]).

In this paper we investigate the conductivity of the distorted electron system (the Peierls distorted system). In Section 2 we describe in the tight binding approximation, a one-dimensional electron model with two atoms per unit cell. Next, in Section 3 we calculated, using the Green function method (see e.g. [4]), the dynamical electrical conductivity. For this simple model the result is exact.

---

* This work was supported by the Polish Academy of Sciences within M.R.-I.9 project.

** Address: Instytut Fizyki Molekularnej PAN, Smoluchowskiego 17/19, 60-179 Poznań, Poland.

2. Distorted one-dimensional electron system in the tight binding approximation

We consider a distorted atomic chain with a half-filled electronic band. In agreement with the Peierls conclusion [5] the period of the distortion is equal to two lattice constants. This situation is shown in Fig. 1. Open circles represent a regular chain with lattice constant

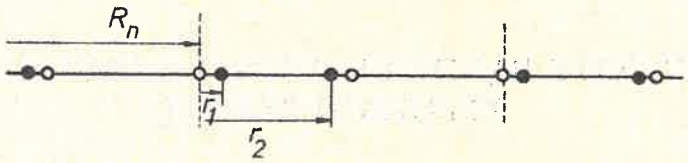

Fig. 1. Distorted chain with one electron per atom

a while full circles — displaced atoms to a distance u. A Hamiltonian of the system in the tight binding approximation is given by

$$H = -\frac{\hbar^2}{2m}\frac{d^2}{dr^2} + \sum_{n,s} V(r-R_n-r_s), \tag{1}$$

where $V(r)$ is an atomic potential, n is the number of the unit cell, while s — the number of the atom inside a cell. The Bloch function is written in the form

$$\psi(r) = \frac{1}{\sqrt{N}} \sum_{n,s} A_{sk} e^{ik(R_n+r_s)} \phi(r-R_n-r_s), \tag{2}$$

where $\phi(r)$ is an atomic function. If we confine calculations to two-center integrals, then the energy E and the coefficients A_{sk} are calculated from the equations

$$\begin{cases} A_{1k}\mu + A_{2k}\frac{1}{2}\left[t_C e^{ik(r_2-r_1)} + t_F e^{ik(r_2-r_1-2a)}\right] = EA_{1k} \\ A_{2k}\mu + A_{1k}\frac{1}{2}\left[t_C e^{-ik(r_2-r_1)} + t_F e^{-ik(r_2-r_1-2a)}\right] = EA_{2k}, \end{cases} \tag{3}$$

where

$$\mu = E_0 + \int dr\phi^*(r-r_1)V(r-r_2)\phi(r-r_1) + \int dr\phi^*(r-r_2)V(r-r_1-2a)\phi(r-r_2) \tag{4}$$

is the crystal field potential (E_0 is an atomic level),

$$t_C = \int dr\varphi^*(r-r_1)V(r-r_2)\phi(r-r_2) \tag{5}$$

is the electron hopping integral between atoms inside a unit cell,

$$t_F = \int dr\phi^*(r-r_2)V(r-r_1-2a)\phi(r-r_1-2a) \tag{6}$$

is the electron hopping integrals between atoms from neighbour unit cells. The results are

$$E_{1(2)}(k) = \mu \pm \{t^2 \cos^2 ka + \delta^2 \sin^2 ka\}^{1/2} \tag{7}$$

and

$$A_{1k} = \frac{1}{\sqrt{2}}, \quad A_{2k} = \pm \frac{1}{\sqrt{2}} \frac{t_C e^{-ik(r_2-r_1)} + t_F e^{-ik(r_2-r_1-2a)}}{|t_C e^{ik(r_2-r_1)} + t_F e^{-ik(r_2-r_1-2a)}|} = \pm \frac{1}{\sqrt{2}} b(k), \tag{8}$$

$$(t = (t_C + t_F)/2, \quad \delta = (t_C - t_F)/2 \text{ and } r_2 - r_1 = a - 2u).$$

In the second quantization we have the function

$$\psi(r) = \sum_{n,s} \phi(r - R_n - r_s) a_{n,s} = \sum_{\substack{k \\ p=1,2}} \psi_{pk}(r) a_{pk}, \tag{9}$$

where $\psi_{pk}(r)$ is the Bloch function

$$\psi_{1(2)k}(r) = \frac{1}{\sqrt{2N}} \sum_n \{e^{ik(R_n+r_1)} \phi(r - R_n - r_1) (\pm) e^{ik(R_n+r_2)} b(k) \phi(r - R_n - r_2)\}. \tag{10}$$

The Hamiltonian

$$H = \sum_n (t_C a^\dagger_{n,1} a_{n,2} + t_F a^\dagger_{n,2} a_{n+1,1}) = \sum_{k,p} E_p(k) a^\dagger_{pk} a_{pk}, \tag{11}$$

describes the distorted electron system in the tight binding approximation. $a_{n,s}$, a_{pk} are annihilation operators of an electron in n-th unit cell and on s-th site, or in the band $p = 1, 2$ with wave vector k, respectively. They transform according to

$$\begin{cases} a_{n,1} = \dfrac{1}{\sqrt{2N}} \displaystyle\sum_k e^{ik(R_n+r_1)} (a_{1k} + a_{2k}) \\ a_{n,2} = \dfrac{1}{\sqrt{2N}} \displaystyle\sum_k e^{ik(R_n+r_2)} b(k) (a_{1k} - a_{2k}). \end{cases} \tag{12}$$

The spin index is neglected everywhere.

The electron dispersion curve given by Eq. (7) is identical with the result obtained for an undistorted chain with modulated hopping integrals [6]. However, only some physical quantities are identical for both models. For example, the dynamical electrical conductivity (given in the next section) depends on the electronic band structure as well as on distances between ions.

The crystallographic structure of NMP-TCNQ is schematically shown in Fig. 2. We consider the central TCNQ chain perpendicular to the plane of the picture. The methyl groups are in positions 1 or 2 and 3 or 4. From X-ray measurments Kobayashi [7] concludes that in NMP-TCNQ crystals there are antiferroelectrically ordered NMP chains. The electrical dipoles are arranged in the perpendicular to the c-axis independent sheets, i.e. in the c-axis direction there are no correlations between them. (However, Morosin [8] asserts that dipole moments in NMP chains are disordered.) Thus, in agreement with Kobayashi's

conclusion, the methyl groups are in the position 1, in the second plane in the position 2, in the position 1 in the next plane and so on.

We suppose that physical properties of NMP-TCNQ depend on the properties of TCNQ chains as well as on their neighbourhoods. The distance from CH_3 in the position 1

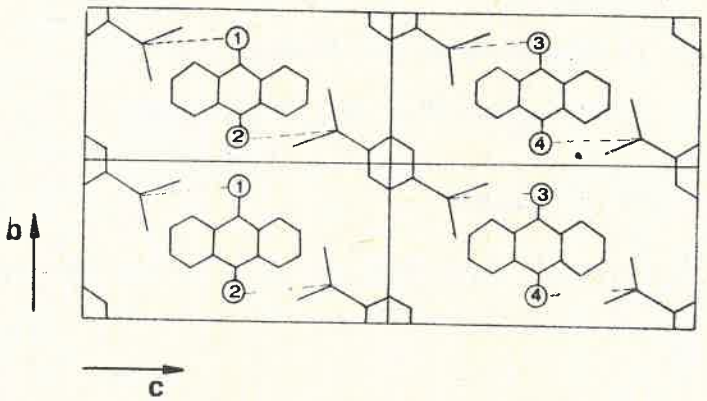

Fig. 2. Schematic crystallographic structure of NMP-TCNQ (the axis of the chains is perpendicular to the plane of the picture). The numbers are placed in the possible configurations of the methyl groups

to the central TCNQ molecule (Fig. 2) is longer than from CH_3 in the position 2 and if the NMP chains are antiferroelectrically orered, we expect, that the electron hopping integrals in TCNQ chain are modulated with a period of two lattice constants.

3. Conductivity of the Peierls distorted system

In this chapter we calculate the dynamical electrical conductivity for the distorted one-dimensional electron model in the tight binding approximation, which is described in the preceeding section. We use the Green function method of Zubarev as described by Smith and Lawson [4]. A current operator is defined by

$$J = -i[P, H], \tag{13}$$

where P is a polarization vector

$$P = e \sum_l X_l a_l^\dagger a_l, \tag{14}$$

($X_l = R_n + r_s$). The perturbation of the system, i.e. the electric field $E = E_0 e^{i\omega t}$, is adiabatically switched on and for the first order perturbation we obtain

$$\langle J(t) \rangle = -\frac{1}{i} \sum_l eE_0 X_l \int_{-\infty}^{\infty} \langle\langle j(t) \, | a_l^\dagger(\tau) a_l(\tau) \rangle\rangle e^{i\omega\tau} d\tau. \tag{15}$$

where $\langle\langle \ldots \mid \ldots \rangle\rangle$ denotes the retarded Green function. Integrating (15) by parts and assuming translation symmetry we may write [4]

$$\langle J(t)\rangle = \frac{eE_0}{i\omega}\int_{-\infty}^{\infty}\left\langle\left\langle j(t)\left|\sum_l X_l \frac{d}{d\tau}(a_l^\dagger(\tau)a_l(\tau))\right\rangle\right\rangle\right. e^{i\omega\tau}d\tau. \tag{16}$$

Using the transformation (12) we have

$$\begin{aligned}\langle J(t)\rangle = \frac{e^2}{i\omega}E_0 e^{i\omega t}\sum_{k,k'}\int_{-\infty}^{\infty} d\tau e^{i\omega\tau}\{&f_1(k,k')\,[G_{1111}+G_{2222}\\ &-G_{1122}-G_{2211}]+f_2(k,k')\,[G_{1112}+G_{2221}-G_{1121}-G_{2212}]\\ &+f_3(k,k')\,[G_{1211}+G_{2122}-G_{2111}-G_{1222}]+f_4(k,k')\,[G_{1212}\\ &+G_{2121}-G_{1221}-G_{2112}]\},\end{aligned} \tag{17}$$

where G denotes Green's function

$$G_{p_1p_2p_3p_4}(k,k';\tau) = \langle\langle a^\dagger_{p_1k}(\tau)a_{p_2k}(\tau)\,|a^\dagger_{p_3k'}a_{p_4k'}\rangle\rangle, \tag{18}$$

$p_i = 1, 2$ are the band indices and f are the functions

$$\begin{aligned} f_1(k,k') &= \alpha(k)\alpha(k'), \quad f_2(k,k') = \alpha(k)\beta(k'),\\ f_3(k,k') &= \beta(k)\alpha(k'), \quad f_4(k,k') = \beta(k)\beta(k'),\end{aligned} \tag{19}$$

where

$$\begin{aligned}\alpha(k) &= -2t_Ct_Fa\sin 2ka/E_k,\\ \beta(k) &= i[t_C^2(a-2u)-t_F^2(a+2u)-4t_Ct_Fu\cos 2ka]/E_k,\end{aligned} \tag{20}$$

and

$$E_k = \{t^2\cos^2 ka+\delta^2\sin^2 ka\}^{1/2}. \tag{21}$$

Using the spectral representation of Green's function we write

$$\langle J(t)\rangle = \frac{ie^2}{\omega}E_0e^{i\omega t}\sum_{\substack{k,k'\\ s}} f_s(k,k')\int_{-\infty}^{\infty}d\tau e^{i\omega\tau}\frac{\theta(\tau)}{i}\int_{-\infty}^{\infty}dE e^{-iE\tau}$$

$$J^{kk'}(E)\,(e^{\beta E}-1) = \frac{ie^2}{\omega}E_0e^{i\omega t}\sum_{\substack{k,k'\\ s}} f_s(k,k')\int_{-\infty}^{\infty}d\tau e^{i\omega\tau}$$

$$\frac{\theta(\tau)}{i}\int_{-\infty}^{\infty}dE(e^{\beta E}-1)\frac{1}{2\pi}\int_{-\infty}^{\infty}dt'e^{iEt'}\langle a_k^\dagger a_{k'}a_k^\dagger(t')a_k(t')\rangle. \tag{22}$$

(We must remember that we sum also on the band indices). The thermodynamical averages, standing after the functions $f_2(k, k')$ and $f_3(k, k')$, are equal zero (see Eqs. (17) and (22)). Using anti-commutator or commutator Green's functions and the relation

$$\langle B(0)A(t)\rangle = \int_{-\infty}^{\infty} \frac{d\omega}{2\pi} \frac{e^{-i\omega t}}{e^{\beta\omega}-\eta} i \lim_{\varepsilon\to 0+} [\langle\langle A|B\rangle\rangle_{\omega+i\varepsilon} - \langle\langle A|B\rangle\rangle_{\omega-i\varepsilon}], \tag{23}$$

(where $\eta = \pm 1$ for a commutator or anti-commutator Green's function, respectively) we calculate the averages standing after $f_1(k, k')$ and $f_4(k, k')$. For example

$$\langle a^{\dagger}_{1k'} a_{2k'} a^{\dagger}_{2k}(t) a_{1k}(t)\rangle = \delta_{k,k'} \frac{n^2_{2k}+n^2_{1k}}{e^{2\beta E_k}+1} e^{-2E_k t}. \tag{24}$$

Finally, we employ the fact that

$$\langle J(t)\rangle = \sigma(\omega) E_0 e^{i\omega t}, \tag{25}$$

and we write the dynamical conductivity in the form

$$\sigma(\omega) = \frac{ie^2}{\omega} \sum_k \left\{ \alpha^2(k) 2n_{2k} n_{1k} \left[P \int_{-\infty}^{\infty} dE \frac{(e^{\beta E}-1)}{\omega+E} \delta(E) + i\pi(e^{\beta\omega}-1)\delta(\omega) \right] \right.$$

$$-\beta^2(k)(n^2_{1k}+n^2_{2k}) \left(\frac{1}{e^{2\beta E_k}+1} \left[P \int_{-\infty}^{\infty} dE \frac{(e^{\beta E}-1)\delta(E-2E_k)}{\omega+E} + i\pi(e^{2\beta E_k}-1)\delta(\omega+2E_k) \right] \right.$$

$$\left. \left. + \frac{1}{e^{-2\beta E_k}+1} \left[P \int_{-\infty}^{\infty} dE \frac{(e^{\beta E}-1)\delta(E+2E_k)}{\omega+E} + i\pi(e^{2\beta E_k}-1)\delta(\omega-2E_k) \right] \right) \right\}, \tag{26}$$

and

$$\mathrm{Re}\,\sigma(\omega) = \frac{\pi e^2}{k_B T} \sum_k \frac{4(t^2-\delta^2)^2 a^2 \sin^2 2ka}{t^2\cos^2 ka + \delta^2 \sin^2 ka} 2n_k(1-n_k)\delta(\omega)$$

$$+ \frac{\pi e^2}{\omega} \sum_k \frac{[(t+\delta)^2(a-2u) - (t-\delta)^2(a+2u) - 4(t^2-\delta^2)u\cos 2ka]^2}{t^2\cos^2 ka + \delta^2 \sin^2 ka}$$

$$\times (2n_k - 1)\,[\delta(\omega-2E_k) - \delta(\omega+2E_k)], \tag{27}$$

where $n_k = \{\exp(-E_k/k_B T)+1\}^{-1}$.

For our simple Hamiltonian (11) we obtained exactly the dy namical electrical conductivity (Eqs. (26) and (27)). The first term of Eq. (27) is the d. c. conductivity ($\omega = 0$). The second one is the optical conductivity ($\omega \neq 0$) and depends of the variation of the hopping

integral δ and on the lattice distortion u. We expect that the dynamical electrical conductivity measurements ($\omega \neq 0$) can provide an answer to the questions: does the Peierls distortion occur or do the surroudings modulate the electron hopping integrals in the TCNQ chains?

We have very similar electron dispersion curves for the case of the distorted chain and for that one, which probably occurs in NMP-TCNQ, where the NMP chains modulate the hopping integrals as well as the atomic level in the TCNQ chain. However, from these calculations (Eq. 27) we see that the a.c. conductivity is different for both cases.

4. Discussion

The NMP-TCNQ crystal has the half-filled electronic band [9] and now we compare the calculated d.c. conductivity with experimental data [10]. We want to emphasize that we only illustrate the usefulness of the calculations presented above. In NMP-TCNQ Coulomb and interchain interactions are strong [1]. The influence of the NMP molecules

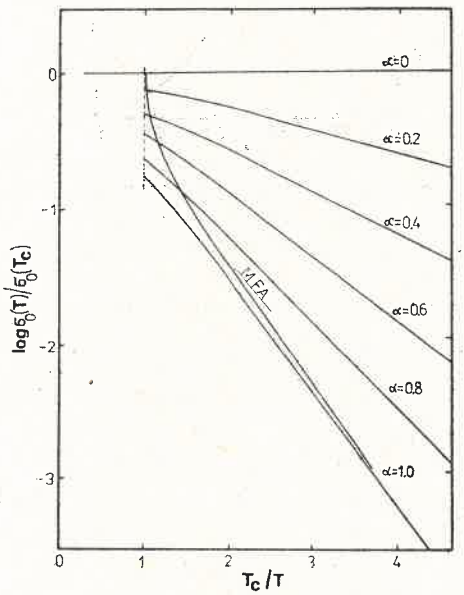

Fig. 3. The d.c. conductivity for the distorted one-dimensional electron system. $\alpha = \delta/\delta_0$, where $\delta_0 = \delta(T = 0)$ is the energy gap determined for zero temperature in the mean field approximation (MFA) [11]

on the TCNQ chain complicates the problem, also. Thus, our model is too simple for an adequate description of this crystal.

Fig. 3 shows the d.c. conductivity (i.e. Re $\sigma(\omega = 0) = \sigma_0(T)$) for different gap parameters $\alpha = \delta/\delta_0$, where $\delta_0 = \delta(T = 0)$ is the gap determined in the mean field approximation, for zero temperature. For constant $\alpha(T)$ we have nearly straight lines, i.e. below a critical temperature, with decreasing temperature the conductivity decreases nearly exponen-

tially. For low temperature, $\delta/k_B \gg 1$, we have an inequality

$$\sigma_0(T) \leqslant \frac{32e^2a^2t}{t^2-\delta^2} \exp\left[-\delta/k_BT\right]. \tag{28}$$

The curve denoted by MFA presents the temperature dependence of the conductivity for the energy gap determined for the Fröhlich model [11] in the mean field approximation. (The MFA gap follows the BCS type temperature dependence [11] — see Fig. 4.)

Fig. 3 may be used as a pattern to determine the temperature dependence of the energy gap. In this figure we draw the experimental points NMP-TCNQ [10] and for a given temperature we read the value of the energy gap α. The results are presented in Fig. 4.

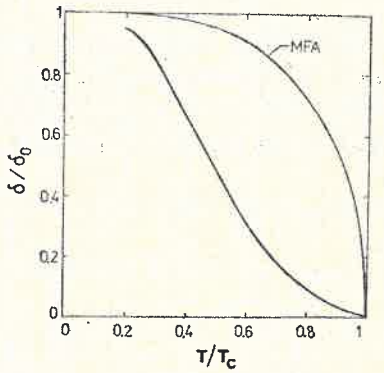

Fig. 4. Temperature dependence of the energy gap of NMP-TCNQ determined from the experimental data of the conductivity [10] and our theoretical calculations for the distorted model. MFA denotes the temperature dependence of the gap calculated for the Fröhlich model in the mean field approximation [11]

This curve has evidently different temperature dependence than the MFA curve. We mentioned above that our model was too simple to claim a description of NMP-TCNQ. We cannot exclude the hypothetical possibility of the non-MFA type temperature dependence of the gap in NMP-TCNQ.

The author would like to express his sincere thanks to Professor J. Morkowski for helpful discussions, for many comments and a critical reading of the manuscript.

REFERENCES

[1] J.-J. André, A. Bieber, F. Gautier, *Ann. Phys.* (France) **1**, 145 (1976).
[2] B. Bułka, *Solid State Commun.* **25**, 101 (1978).
[3] J.-L. Calais, *Int. J. Quantum Chem.* **11**, 547 (1977).
[4] R. C. Smith, J. O. Lawson, *Physica* **83A**, 505 (1976).
[5] R. E. Peierls, *Quantum Theory of Solids*, Oxford University Press, London 1955.
[6] L. N. Bulaevski, *Usp. Fiz. Nauk* **115**, 263 (1975).
[7] H. Kobayashi, *Bull. Chem. Soc. Japan* **48**, 1373 (1975).
[8] B. Morosin, *Phys. Lett.* **A53**, 455 (1975).
[9] M. A. Butler, F. Wudl, *Phys. Rev.* **B12**, 4708 (1975).
[10] A. J. Epstein, E. M. Conwell, D. J. Sandman, J. S. Miller, *Solid State Commun.* **23**, 355 (1977).
[11] See for example: M. J. Rice, S. Strässler, *Solid State Commun.* **13**, 125 (1973).